Molecular Physics, 1989, Vol. 66, No. 2, 429–456

First principles calculation of rotational and ro-vibrational line strengths

Spectra for H_2D^+ and D_2H^+

by STEVEN MILLER and JONATHAN TENNYSON
Department of Physics and Astronomy, University College London,
Gower Street, London WC1E 6BT, England

and BRIAN T. SUTCLIFFE
Department of Chemistry, University of York,
York YO1 5DD, England

(*Received 2 August 1988; accepted 5 October 1988*)

Theory is developed for the calculation of dipole transition line strengths and frequencies for rotational and ro-vibrational transitions from wavefunctions expressed in the generalized body-fixed co-ordinates proposed by Sutcliffe and Tennyson (1986, *Molec. Phys.*, **58**, 1053). Computations using this theory produce calculated frequencies for the fundamental ro-vibrational transitions of H_2D^+ and D_2H^+ in very good agreement with experiment. These first principles calculations use the highly accurate *ab initio* electronic potential energy and dipole surface of Meyer, Botschwina and Burton, which has previously been shown by the authors to give ro-vibrational transition frequencies, rotational constants and vibrational fundamentals of spectroscopic accuracy. Three line reassignments are proposed on frequency considerations. Several transitions are proposed as candidates for observation on the grounds of computed relative intensities. Calculated pure rotational transitions in ground state for H_2D^+ and D_2H^+ are in excellent agreement with limited data available, and the full rotational spectra of these molecules are predicted.

1. Introduction

Recent advances in experimental techniques have enabled the infrared and microwave spectra of many new species to be measured. In particular, there is currently great interest in molecular ions which have not only laboratory and industrial relevance, but are considered to be important in understanding the chemical pathways in the interstellar gas clouds which occupy vast regions of the galaxy.

One such molecular ion is H_3^+, whose infrared spectrum was first measured by Oka in 1980 [1]. Since then there have been several spectroscopic studies not only of H_3^+ itself, but of its deuterated isotopomers D_3^+, first observed at the same time as H_3^+ by Shy *et al.* [2], H_2D^+ and D_2H^+, in the infrared region [3–10]. H_3^+ has an equilibrium geometry which is an equilateral triangle, giving H_3^+ and D_3^+ D_{3h} symmetry, and H_2D^+ and D_2H^+ C_{2v} symmetry.

For the D_{3h} triatomics the only fundamental which is infrared active is the degenerate ν_2 mode. The absence of a permanent dipole means that, in the standard approximation, pure rotational transitions are 'forbidden'. The possibility of detecting these 'forbidden' rotational spectrum has been discussed elsewhere [11, 12].

All three fundamental vibrations, ν_1, ν_2 and ν_3, are infrared active for H_2D^+ and

0026–8976/89 $3.00

D_2H^+. Since there is a permanent dipole in the ground state, due to the non-coincidence of the centre of charge and the centre of mass, there is also the possibility of observing pure rotational transitions. To date, however, only three lines of the H_2D^+ spectrum have been measured [13–16], and one of D_2H^+ [16].

As well as the experimental investigations, there have been several theoretical studies of the ro-vibrational energy levels of these molecules spanning a period of 15 years [17–24], using a number of different *ab initio* potential energy surfaces [17, 25–27].

In the last few years, we have employed a potential due to Meyer *et al.* (MBB) [27] which has proved extremely accurate for calculations of the vibrational fundamentals. Our studies showed that it also gave excellent results for the rotational energy levels and constants of all four molecules in comparison with experiment [24]. We have used the MBB potential to predict ro-vibrational energy levels in the overtone manifolds of H_3^+ up to $3\nu_2$ [28], and these have led to the successful identification of both overtone [29] and 'hot band' [30] transitions.

One vital piece of information which can be furnished by theoretical studies, but which is difficult to extract from the experimental measurements made so far, is a set of accurate line strengths for the rotational or ro-vibrational transitions of interest. In this paper we generalize the theory developed by Brocks *et al.* [31] for the calculation of line strengths from the wavefunction generated by the method of Sutcliffe and Tennyson (ST) [19, 23].

We present comparisons of transition frequencies for the infrared fundamentals of H_2D^+ and D_2H^+ with those measured experimentally alongside the predicted line strengths. Calculated frequencies and line strengths for the pure rotational ground state transitions are also given.

2. Theory

The ST method employs a generalized system of internal molecular co-ordinates [23], distances r_1 and r_2, and the angle between them, θ. In scattering co-ordinates, r_1 is the bond between two of the atoms and r_2 is the line joining the midpoint of r_1 and the third atom. In bond-length/bond-angle co-ordinates [32], two bonds and the included angle are chosen. Other choices are also possible [23]. The ro-vibrational wavefunctions computed in this method are expanded in terms of a basis set which consists of products of angular and radial functions.

The angular functions chosen are the Condon and Shortley $\Theta_{jk}(\theta)$ functions, coupled with the usual Wigner rotation matrices $D^J_{Mk}(\alpha, \beta, \gamma)$ [33]. The total angular momentum is given by J, with k its projection on the body-fixed z-axis. The wavefunctions are symmetrized according to the usual Wang operators, using the symmetry quantum number p which can take on the valuess of 0 or 1. With this symmetrization k is then set to $|k|$, with $p \leqslant k \leqslant J$. The wavefunction has an overall parity given by $(-1)^{J+p}$. The subscript M spans the magnetic sub-levels of the wavefunction. The angular basis set if then given by

$$\begin{aligned} |J_M, k, j, p\rangle &= \left(\frac{2J+1}{8\pi^2}\right)^{1/2} \Theta_{j0}(\theta) D^{*J}_{M0}(\alpha, \beta, \gamma), \quad k = 0, p = 0; \\ &= (-1)^k \left(\frac{2J+1}{8\pi^2}\right)^{1/2} (1/2)^{1/2} \{\Theta_{jk}(\theta) D^{*J}_{M-k}(\alpha, \beta, \gamma) \\ &\quad + (-1)^p \Theta_{j-k}(\theta) D^{*J}_{Mk}(\alpha, \beta, \gamma)\}, \quad k > 0, p = 0, 1. \end{aligned} \tag{1}$$

The radial part of the wavefunction is represented by $\phi_m(r_1)\phi_n(r_2)$, which can be Morse-oscillator-like functions or other suitable radial functions [19]. We define

$$|n, m\rangle = \phi_m(r_1)\phi_n(r_2). \tag{2}$$

Then the lth eigenfunction of the Jth angular momentum level with parity p is given by:

$$\begin{aligned} |J_M, p, l\rangle &= \sum_{k=p}^{J} \sum_{jmn} d_{kjmn}^{JMpl} |J_M, k, j, p\rangle |m, n\rangle \\ &= \sum_{k=p}^{J} \sum_{jmn} d_{kjmn}^{JMpl} \times |J_M, k, j, m, n, p\rangle. \end{aligned} \tag{3}$$

The line strength $S(f-i)$ of a particular transition from initial state i to a final state f is given by

$$S(f-i) = \sum_{M'M''\tau} (T_{if}^{M'M''\tau})^2, \tag{4}$$

where

$$T_{if}^{M'M''\tau} = \langle J'_{M'}, p', l' | \mu_\tau^s | J''_{M''}, p'', l''\rangle \tag{5}$$

and μ_τ^s is the τ component of the space-fixed dipole moment.

In the ST method, the molecular z-axis is fixed along either r_1 or r_2, and the x-axis perpendicular to z in the plane of the molecule. For a triatomic molecule, therefore, only the z and x components of the body-fixed dipole moment are non-zero.

Following Brocks *et al.* [31] we expand the molecular body-fixed dipole:

$$\mu_z^m(r_1, r_2, \theta) = \sum_{\lambda=0} B_{\lambda,0}(r_1, r_2) P_\lambda^0(\cos\theta) \tag{6}$$

and

$$\mu_x^m(r_1, r_2, \theta) = \sum_{\lambda=1} B_{\lambda,1}(r_1, r_2) P_\lambda^1(\cos\theta). \tag{7}$$

It is convenient to define

$$\begin{aligned} \mu_\nu^m(r_1, r_2, \theta) &= \sum_{\lambda=0} \left(\frac{2}{2\lambda+1}\right)^{1/2} B_{\lambda,0}(r_1, r_2)\Theta_{\lambda,0}(\theta), && \nu = 0; \\ &= \sum_{\lambda=1} \left(\frac{1}{2\lambda+1}\right)^{1/2} [\lambda(\lambda+1)]^{1/2} B_{\lambda,\nu}(r_1, r_2)\Theta_{\lambda,\nu}(\theta), && \nu = \pm 1, \end{aligned} \tag{8}$$

with $B_{\lambda,-1}(r_1, r_2) = B_{\lambda,+1}(r_1, r_2)$ for all values of λ.

The relation between $\Theta_{\lambda,\nu}(\theta)$ and the (associated) Legendre polynomials used to expand the cartesian components of the body-fixed dipole may be obtained via the spherical harmonic $Y_{\lambda,\nu}(\theta, 0)$ according to the definition used by Brink and Satchler [33]. This leads to

$$\mu_0^m(r_1, r_2, \theta) = \mu_z^m(r_1, r_2, \theta), \tag{9}$$

and

$$\mu_{\pm 1}^m(r_1, r_2, \theta) = \mp (1/2)^{1/2} \mu_x^m(r_1, r_2, \theta). \tag{10}$$

The body-fixed dipole moment, $\boldsymbol{\mu}^{\mathrm{m}}(r_1, r_2, \theta)$, transforms as a tensor of rank one into space-fixed co-ordinates [31] and we can therefore write

$$\mu_\tau^{\mathrm{s}} = \sum_{\nu=-1}^{+1} \mu_\nu^{\mathrm{m}}(r_1, r_2, \theta) D_{\tau,\nu}^{*1}(\alpha, \beta, \gamma). \tag{11}$$

The individual components $T_{if}^{M'M''\tau}$ may now be calculated from

$$\begin{aligned} T_{if}^{M'M''\tau} &= \langle J'_{M'}, p', l' \,|\, \mu_\tau^{\mathrm{s}} \,|\, J''_{M''}, p'', l'' \rangle \\ &= \sum_{\nu=-1}^{+1} \sum_{k'=p'}^{J'} \sum_{j'm'n'} \sum_{k''=p''}^{J''} \sum_{j''m''n''} \\ &\quad \times \langle J'_{M'}, k', j', m', n', p' \,|\, \mu_\nu^{\mathrm{m}} D_{\tau,\nu}^{*1} \,|\, J''_{M''}, k'', j'', m'', n'', p'' \rangle. \end{aligned} \tag{12}$$

The expansion of the dipole moment given in equation (8) coupled with the explicit form of the wavefunction in equation (3) means that the radial and angular integrals in equation (12) may be evaluated separately. Taking the radial integrals first, we may define

$$B_{\lambda,\nu}^{m'm''n'n''} = \langle m', n' \,|\, B_{\lambda,\nu}(r_1, r_2) \,|\, m'', n'' \rangle. \tag{13}$$

Turning to the angular integration, it is possible to separate this into those parts involving the integral angle θ and those involving the Wigner angles α, β, γ. Using the conventions of Brink and Satchler [33] and allowing for the phase factors introduced by the ST choice of basis functions, we have

$$\begin{aligned} &\sum_{\nu=-1}^{1} \sum_{\lambda=|\nu|} \sum_{k''=p''}^{J''} \sum_{k'=p'}^{J'} \sum_{j''j'} d_{k'j'm'n'}^{J'M'p'l'} d_{k''j''m''n''}^{J''M''p''l''} \\ &\quad \times \langle J'_{M'}, k', j', p' \,|\, \Theta_{\lambda,\nu}(\theta) D_{\tau,\nu}^{*1}(\alpha, \beta, \gamma) \,|\, J''_{M''}, k'', j'', p'' \rangle \\ &= \frac{(-1)^{M'}}{2} [(2J'+1)(2J''+1)]^{1/2} \\ &\quad \times \sum_{\nu=-1}^{1} \sum_{\lambda=|\nu|} \sum_{k''=p''}^{J''} \sum_{k'=p'}^{J'} \sum_{j''j'} a(\nu, \nu+k'', \lambda)[(2j'+1)(2j''+1)]^{1/2} \\ &\quad \times \begin{pmatrix} J' & 1 & J'' \\ -M' & \tau & M'' \end{pmatrix} \times \left[\begin{pmatrix} J' & 1 & J'' \\ k' & \nu & -k'' \end{pmatrix} \begin{pmatrix} j' & \lambda & j'' \\ 0 & 0 & 0 \end{pmatrix} \begin{pmatrix} j' & \lambda & j'' \\ k' & \nu & -k'' \end{pmatrix} \right. \\ &\quad \left. + (-1)^{p''+p'} \begin{pmatrix} J' & 1 & J'' \\ -k' & \nu & k'' \end{pmatrix} \begin{pmatrix} j' & \lambda & j'' \\ 0 & 0 & 0 \end{pmatrix} \begin{pmatrix} j' & \lambda & j'' \\ -k' & \nu & k'' \end{pmatrix} \right] d_{k'j'm'n'}^{J'M'p'l'} d_{k''j''m''n''}^{J''M''p''l''} \\ &= \frac{(-1)^{M'}}{2} [(2J'+1)(2J''+1)]^{1/2} \\ &\quad \times \sum_{\nu=-1}^{1} \sum_{\lambda=|\nu|} \sum_{k''=p''}^{J''} \sum_{k'=p'}^{J'} \sum_{j''j'} a(\nu, \nu+k'', \lambda)[(2j'+1)(2j''+1)]^{1/2} \\ &\quad \times \begin{pmatrix} J' & 1 & J'' \\ -M' & \tau & M'' \end{pmatrix} \begin{pmatrix} J' & 1 & J'' \\ -k' & \nu & k'' \end{pmatrix} \begin{pmatrix} j' & \lambda & j'' \\ 0 & 0 & 0 \end{pmatrix} \begin{pmatrix} j' & \lambda & j'' \\ -k' & \nu & k'' \end{pmatrix} \\ &\quad \times d_{k'j'm'n'}^{J'M'p'l'} d_{k''j''m''n''}^{J''M''p''l''} \times [(-1)^{J''+J'+1} + (-1)^{p''+p'}], \end{aligned} \tag{14}$$

where the second expression is obtained by manipulation of the $3-j$ symbols and reordering the summation over ν. (Note that there is no phase dependence on $(-1)^{j''+\lambda+j'}$ since this must be even for the integrals not to vanish.)

In equation (14)

$$\begin{aligned}
a(0, n, \lambda) &= 1, \qquad 0 \leqslant n \leqslant J', \\
a(\pm 1, 0, \lambda) &= -[\lambda(\lambda+1)]^{1/2}, \\
a(\pm 1, n, \lambda) &= -[\lambda(\lambda+1)/2]^{1/2}, \quad 0 < n \leqslant J', \\
a(v, n, \lambda) &= 0, \quad n < 0, \quad n > J', \quad v = 0, \pm 1.
\end{aligned}$$

The rules governing the $3-j$ symbols mean that the v components of the dipole moment couple basis functions with angular momentum projection $k'' = k$ to those with $k' = k + v$. Equations (11)–(14) then give

$$\begin{aligned}
T_{if}^{M'M''\tau} = {} & \frac{(-1)^{M'}}{2}[(2J'+1)(2J''+1)]^{1/2}\begin{pmatrix} J' & 1 & J'' \\ -M' & \tau & M'' \end{pmatrix} \\
& \times \sum_{v=-1}^{+1} \sum_{\lambda=|v|} \sum_{k=p''}^{J''} \sum_{j''j'} a(v, v+k, \lambda)[(2j'+1)(2j''+1)]^{1/2} \\
& \times \begin{pmatrix} J' & 1 & J'' \\ -k-v & v & k \end{pmatrix}\begin{pmatrix} j' & \lambda & j'' \\ 0 & 0 & 0 \end{pmatrix}\begin{pmatrix} j' & \lambda & j'' \\ -k-v & v & k \end{pmatrix} \\
& \times \sum_{m''n''} \sum_{m'n'} B_{\lambda, v}^{m'm''n'n''} \times d_{k'j'm'n'}^{J'M'p'l'} d_{k''j''m''n''}^{J''M''p''l''}[(-1)^{J''+J'+1} + (-1)^{p''+p''}]. \qquad (15)
\end{aligned}$$

This equation is a generalization of the result obtained by Brocks *et al.* [31], which was valid only for $J \leqslant 1$.

In practice, the individual magnetic components of the wavefunctions are not computed separately. Summing over these then gives

$$\begin{aligned}
S(f-i) = {} & \tfrac{1}{4}[(2J'+1)(2J''+1)] \\
& \times \Bigg[\sum_{v=-1}^{+1} \sum_{\lambda=|v|} \sum_{k=p''}^{J''} \sum_{j''j'} a(v, v+k, \lambda)[(2j'+1)(2j''+1)]^{1/2} \\
& \times \begin{pmatrix} J' & 1 & J'' \\ -k-v & v & k \end{pmatrix}\begin{pmatrix} j' & \lambda & j'' \\ 0 & 0 & 0 \end{pmatrix}\begin{pmatrix} j' & \lambda & j'' \\ -k-v & v & k \end{pmatrix} \\
& \times \sum_{m''n''} \sum_{m'n'} B_{\lambda, v}^{m'm''n'n''} \times d_{k'j'm'n'}^{J'p'l'} d_{k''j''m''n''}^{J''p''l''}[(-1)^{J''+J'+1} + (-1)^{p''+p'}] \Bigg]^2. \\
& \qquad (16)
\end{aligned}$$

The sum rules applying to the $3-j$ symbols in equation (16) and the phase factors at the end of the equation impose the selection rules for all molecular symmetries

$$\Delta J = 0, \quad \Delta p = \pm 1; \quad \Delta J = \pm 1, \quad \Delta p = 0.$$

Additional selection rules which depend on specific molecular symmetries arise as a result of the structure of the wavefunction computed from the basis functions.

Values for the integrated absorption coefficient may be obtained from [18]

$$I(\omega_{if}) = \frac{8\pi N_A \omega_{if} g_i \exp(-E''/kT)[1 - \exp(hc\omega_{if}/kT)]}{3hQ} S(f-i) \qquad (17)$$

where N_A is Avagadro's number (this may be replaced by the relevant number density if comparison with a specific experiment is required), ω_{if} is the transition frequency in cm^{-1}, g_i is the spin-plus-symmetry degeneracy of the initial state, E'' is the energy of the initial state, h is Planck's constant, k is Boltzmann's constant, T is the temperature, and the partition function, Q, is given by

$$Q = \sum_i g_i(2J_i + 1) \exp(-E_i/kT). \tag{18}$$

The Einstein A_{if} coefficient for spontaneous emission is given by

$$A_{if} = \frac{1}{(2J_f + 1)} \frac{64\pi^2\omega_{if}^3}{3h} S(f - i). \tag{19}$$

3. Computational details

For this study of H_2D^+ and D_2H^+ we used the corrected MP-7/87CGTO potential energy and dipole surfaces of Meyer *et al.* [27]. The co-ordinate system chosen was the scattering co-ordinates used in our previous study [24] of these molecules, with the molecular z-axis fixed along r_2 for H_2D^+ and along r_1 for D_2H^+.

Eigenvalues and wavefunctions were calculated using the suite of programs TRIATOM, SELECT and ROTLEVD. Full details of the first two programs, as well as most of those of ROTLEVD, have been given elsewhere [35]. There have been a number of refinements to this program suite in the past few years [36], and an updated version will be published shortly [37]. These calculations employ the two-step variational technique of Tennyson and Sutcliffe (see, for example, [34]).

The first step in this approach is to operate on the basis functions given in equations (1)–(3) with only that part of the ro-vibrational hamiltonian which does not couple states with different values of k. This is equivalent to ignoring off-diagonal Coriolis interactions. An intermediate set of basis functions is obtained

$$|J, k, p, i\rangle = \sum_{jmn} c_{jmn}^{Jkpi} |J, k, j, m, n, p\rangle. \tag{20}$$

In the second step, the full hamiltonian, including Coriolis coupling of states with k to $k \pm 1$, operates on this intermediate basis set to produce the final ro-vibrational wavefunctions and eigenenergies. This gives

$$\begin{aligned} |J, p, l\rangle &= \sum_{ki} b_{ki}^{Jpl} |J, k, p, i\rangle \\ &= \sum_{ki} \sum_{jmn} b_{ki}^{Jpl} c_{jmn}^{Jkpi} |J, k, m, j, n, p\rangle. \end{aligned} \tag{21}$$

From this it can be seen that

$$d_{kjmn}^{Jpl} = \sum_i b_{ki}^{Jpl} c_{jmn}^{Jkpi}. \tag{22}$$

The size of the initial and intermediate basis sets used is controlled by input parameters to the programs which set the upper limits of the sums over j, m and n in the first step, and i in the second. Not all the possible combinations of j, m and n are, in practice, necessary to converge the first step. Instead N_{Sel} may be chosen on the basis of their energy ordering for particular values of J, k and p [34]. Usually the $J = 0$, $k = 0$ set is used for this purpose.

Nor are all the solutions of the first step necessarily needed fully to converge the second step. The set of intermediate basis functions may be curtailed either by selecting the N_k functions with lowest energy for each k subset, or by selecting the N with lowest energy, irrespective of the value of k. In the first case, N_k is the same for each k subset, but this is not necessarily so for the second selection procedure.

In computing the wavefunctions and eigenenergies for H_2D^+ and D_2H^+ we set the maximum values of m and n to 10, and of j to 24 (j even) or 25 (j odd). Of these, the 600 j, m, n combinations which gave the lowest eigenergies for $J = 0$, $k = 0$, j even were used to generate the $|J, K, j, m, n, p\rangle$ used in the first step. The final wavefunctions, $|J, p, l\rangle$, were computed from the intermediate basis set obtained by taking the 300 lowest $|J, k, p, i\rangle$ for each k subset. The final eigenenergies were converged to 0·1 cm^{-1}, or better, for the energy levels considered up to $J = 10$, with the $J = 0$ levels converged to 0·001 cm^{-1}.

The two different upper limits for the cases of j even or odd arise because the ST method computes the eigenvalues and wavefunctions arising from these basis functions in separate calculations for molecules with C_{2v} symmetry or greater. The j even calculations correspond to *para*-H_2D^+ and *ortho*-D_2H^+, with the nuclear spin weightings, g_{ns}, of 1 and 6 respectively. The j odd calculations give the *ortho*-H_2D^+ and *para*-D_2H^+ wavefunctions, with $g_{\mathrm{ns}} = 3$ in both cases.

The transition moments, line strengths, Einstein A-coefficients and intensities were computed using two new members of the TRIATOM program suite, DIPOLE and SPECTRA, which will be published shortly [37]. DIPOLE is directly driven from input generated either by ROTLEVD or TRIATOM and stored on disk. Output from DIPOLE and energy levels from ROTLEVD/TRIATOM drive SPECTRA.

DIPOLE has many features in common with that part of TRIATOM which computes integrals over the potential energy surface, the main difference being due to the vector nature of the dipole surface as against the scalar potential.

As is the case with their potential energy surface, the MBB dipole surface is expressed in symmetry-adapted, Morse-like co-ordinates. In order to use it to compute transition moments, the dipole surface has first to be transformed to the scattering co-ordinates used to calculate the wavefunctions, and then expanded as a sum of (associated) Legendre functions, thus

$$B_{\lambda,\nu}(r_1, r_2) = \left(\frac{2\lambda+1}{2}\right)\frac{(\lambda-\nu)!}{(\lambda+\nu)!}\int_{-1}^{1} \mu_\chi^m(r_1, r_2, u) P_\lambda^\nu(u)\, du, \tag{23}$$

with $\nu = 0$, $\chi = z$, and $\nu = 1$, $\chi = x$.

In any computational procedure, it is clear that the integrand can only be evaluated at a finite number of points. For the potential energy surface expansion, Gauss–Legendre integration [38] has proved highly accurate [35]. In order to obtain good convergence for the expansion of the dipole surface (equations (6) and (7)), however, we used a Gauss–Jacobi quadrature system [38]. This replaces the integral in equation (23) by a series, thus

$$\int_{-1}^{1} (1-u)^\alpha (1+u)^\beta f_\nu(u)\, du = \sum_{i=1}^{L} A_{\nu i} f_\nu(u_i), \tag{24}$$

where

$$f_\nu(u) = \frac{\mu_\chi^m(r_1, r_2, u) P_\lambda^\nu(u)}{(1-u)^\alpha (1+u)^\beta}. \tag{25}$$

and ν and χ are related as in equation (23).

We used the routines given by Stroud and Secrest [38] to compute the integration points, u_i, and weights, A_i, with $\alpha = \beta = \nu$. Replacing u by $\cos\theta$ then gives

$$f_\nu(\cos\theta) = \frac{\mu_\chi^m(r_1, r_2, \cos\theta)P_\lambda^\nu(\cos\theta)}{(\sin\theta)^{2\nu}}. \tag{26}$$

This form of $f_\nu(u)$ removes all of the factors of $\sin\theta$ which occur in the dipole expansion, ensuring a series which converges rapidly with increasing L for both components of the dipole surface.

In practice we used $L = 2\lambda_{\max} + 1$, where $\lambda_{\max} = 2j_{\max}$ and $j_{\max}$ was the largest value of j chosen, as this guaranteed accurate integrals [39]. For the radial coordinates we used 21-point Gauss–Laguerre quadrature, which has previously been shown to be more than adequate for the MBB potential energy surface [24]. Using these integration schemes, all the transition moments were converged to at least three significant figures for states up to $J = 10$.

All the data presented in the next section were computed on the Cray XMP/48 at the Atlas Computing Centre at the Science and Engineering Research Council's Rutherford Appleton Laboratories.

4. Results

The rotational and ro-vibrational spectra of H_2D^+ and D_2H^+ are extremely rich since the possibility of observing transitions is governed by propensity considerations rather than strict selection rules. For states with $J \leqslant 10$, we have computed more than 24 000 line strengths for each molecule.

These lines include pure rotational transitions in excited vibrational states, overtone ro-vibrational bands and 'hot bands'. In this paper, however, we present only the ro-vibrational transitions to the fundamental vibrational manifolds and the pure rotational spectrum in the ground state for both molecules.

One advantage of theoretical calculations over experimentally measured spectra is that full knowledge can be obtained of the quantum numbers associated with any transition. This can be important where, as there is in the case of both H_2D^+ and D_2H^+, there is some dispute as to the assignment of certain observed lines [10].

Table 1 shows the band origins for the three fundamental transitions for H_2D^+ and D_2H^+ obtained in our $J = 0$ calculations compared with those obtained from the experimental data. The MBB potential was optimized to obtain very good agreement with the ν_2 band origin of H_3^+, and this is reflected in the extremely good agreement between the calculated and experimental values for both molecules. Only the ν_3 mode of D_2H^+ differs by more than $0{\cdot}5\,\mathrm{cm}^{-1}$ from the experimental value.

In order to make the amount of data presented here manageable, we have included transitions in our tables on the basis of their intensity relative to the maximum observed in the spectral region of interest, $I_{\mathrm{Rel}}(\omega)$, at appropriate temperatures.

Calculated ro-vibrational transitions for the ν_2/ν_3 and ν_1 manifolds for H_2D^+ are given in tables 2 and 3 respectively. Foster *et al.* [9], estimate the temperature at which their ν_2/ν_3 data was obtained at about 200 K.

For this manifold we have therefore included all transitions whose calculated relative intensities at 200 K are greater than 0·01. In addition, we have also included all those weaker lines which have been experimentally observed. For ν_1 (table 3), the

Table 1. Calculated and measured vibrational fundamentals for H_2D^+ and D_2H^+ (units cm^{-1}).

	H_2D^+			D_2H^+		
Mode	Calculated	Observed	Obs.–calc.	Calculated	Observed	Obs.–calc.
ν_2	2206.244	2205.869[a]	-0.375	1967.825	1968.170[b]	0.345
ν_3	2334.986	2335.449[a]	0.463	2079.212	2078.410[b]	-0.802
ν_1	2992.962	2992.505[c]	-0.457	2737.302	2736.941[c]	-0.361

[a] Reference 6.
[b] Reference 9.
[c] Reference 10.

cut-off was $I_{Rel}(\omega) \geqslant 0{\cdot}1$, and the temperature was set to 300 K to include more, rather than fewer, transitions.

For the ν_2/ν_3 transitions, the 73 lines for which comparison with experiment was possible gave a root mean square (r.m.s.) deviation between the calculated and experimental lines of $0{\cdot}388\,cm^{-1}$. On more detailed examination, the difference between observed and calculated results, $\Delta\omega_{o-c}(=\omega_{if}(\text{observed}) - \omega_{if}(\text{calculated}))$, is almost uniformly negative for ν_2 and positive for ν_3, in line with the differences in band origins.

Similarly, the ν_1 calculations—for which the r.m.s. deviation on 37 lines is $0{\cdot}421\,cm^{-1}$—consistently overestimate the line frequencies. But for all three modes, when the difference in band origins are taken into account, almost all the calculated transitions lie with $\pm 0{\cdot}2\,cm^{-1}$ of those measured experimentally.

The D_2H^+ manifolds (tables 4 and 5) show very similar behaviour. The r.m.s. deviations are $0{\cdot}400\,cm^{-1}$ (86 lines) and $0{\cdot}281\,cm^{-1}$ (34 lines) for ν_2/ν_3 and ν_1 respectively. Relative intensities for the former manifold were calculated at 150 K (in line with experimental assumptions), while ν_1 intensities were again calculated at 300 K.

For both molecules, there are a number of experimentally measured lines—especially at lower frequencies in the ν_2/ν_3 manifolds—which one would not expect to be observable on the basis of the relative intensities calculated at the temperatures estimated. At the same time, our calculations predict a number of transitions to be measureable which have not, so far, been reported.

It is clear, however, that the vast majority of observed lines also correspond to those calculated to be the most intense. We thus consider that the disparity between the calculated intensities and the observed lines to be a product of the difficulty of obtaining uniform experimental conditions (i.e. a Boltzmann distribution of energies and uniform sensitivity across the spectral range) rather than a failure of either the theory presented above or the MBB dipole surface.

In re-examining the data for the ν_1 manifolds, Kozin *et al.* [10] made a number of line reassignments on the basis of fitting the data to the relevant phenomenological hamiltonians. Our results confirm their reassignments, with the exception of the D_2H^+ ν_1 line at $2990{\cdot}154\,cm^{-1}$, which we have assigned back to its original designation of $4_{40} - 3_{31}$ on consideration of frequency.

It is interesting to consider the H_2D^+ ν_1 line occurring at $3168{\cdot}702\,cm^{-1}$, which Kozin *et al.* reassigned from $5_{12} - 4_{14}$ to $5_{05} - 4_{04}$, (labelled *e* in table 3). Our

Table 2. Calculated and observed ν_2 and ν_3 transitions for H_2D^+. Relative intensities calculated at 200 K.

Mode	$J'K'_aK'_c$	$J''K''_aK''_c$	E''/ cm^{-1}	ω_{if}(calc.)/ cm^{-1}	ω_{if}(obs.)^a/ cm^{-1}	$\Delta\omega_{o-c}$/ cm^{-1}	$S(f-i)^b$/ D^2	$I_{Rel.}(\omega)^c$
ν_2	6 1 5	7 1 6	1272.962	1837.821	1837.573^d	-.248	.151(+0)	.000
ν_2	6 2 5	7 2 6	1273.635	1837.938	1837.688^d	-.250	.153(+0)	.000
ν_2	5 0 5	6 0 6	801.430	1892.818	1892.541^d	-.277	.164(+0)	.004
ν_2	5 1 5	6 1 6	801.484	1892.837	1892.558^d	-.279	.164(+0)	.011
ν_2	5 1 4	6 1 5	990.739	1896.266	1895.995^d	-.271	.110(+0)	.002
ν_2	5 2 4	6 2 5	992.945	1896.621	1896.345^d	-.276	.114(+0)	.001
ν_2	4 1 3	5 1 4	738.472	1952.328	1952.024^d	-.304	.703(-1)	.007
ν_2	4 0 4	5 0 5	586.049	1954.182	-	-	.122(+0)	.013
ν_2	4 1 4	5 1 5	586.266	1954.262	-	-	.122(+0)	.039
ν_2	3 1 2	4 1 3	515.930	2004.514	-	-	.376(-1)	.020
ν_2	3 0 3	4 0 4	402.725	2012.933	2012.621	-.312	.817(-1)	.033
ν_2	3 1 3	4 1 4	403.529	2013.322	2013.010	-.312	.831(-1)	.100
ν_2	2 1 1	3 1 2	326.011	2053.606	2053.211	-.395	.179(-1)	.039
ν_3	3 2 2	4 3 1	654.321	2055.441	-	-	.597(-1)	.012
ν_2	2 2 1	3 2 2	354.677	2061.082	2060.684	-.396	.222(-1)	.013
ν_2	2 0 2	3 0 3	251.316	2067.300	2066.958	-.342	.453(-1)	.056
ν_2	2 1 2	3 1 3	253.969	2069.023	2068.680	-.343	.480(-1)	.175
ν_3	3 2 1	4 3 2	645.411	2071.355	-	-	.769(-1)	.017
ν_2	4 1 4	3 3 1	458.283	2082.246	2081.851	-.395	.648(-4)	.000
ν_2	1 1 0	2 1 1	175.859	2102.906	2102.488	-.418	.762(-2)	.050
ν_3	2 2 1	3 3 0	459.763	2108.250	2108.633	.383	.930(-1)	.079
ν_3	2 2 0	3 3 1	458.283	2110.820	2111.226	.406	.994(-1)	.085
ν_3	2 1 2	3 2 1	376.204	2114.408	-	-	.211(-1)	.011
ν_2	1 0 1	2 0 2	131.594	2115.424	2115.046	-.378	.186(-1)	.056
ν_2	1 1 1	2 1 2	138.815	2120.317	2119.938	-.379	.196(-1)	.168
ν_3	2 1 1	3 2 2	354.677	2157.287	2157.701	.414	.557(-1)	.034
ν_2	0 0 0	1 0 1	45.678	2160.571	2160.176	-.395	.557(-2)	.032
ν_3	1 1 1	2 2 0	223.813	2178.542	-	-	.430(-1)	.068
ν_2	1 1 1	1 1 0	72.433	2186.699	2186.344	-.355	.157(-2)	.022
ν_3	1 1 0	2 2 1	218.620	2190.231	2190.664	.433	.614(-1)	.102
ν_3	4 0 4	5 1 5	586.266	2190.521	-	-	.762(-1)	.027

Table 2 (*continued*).

Mode	$J'K'_aK'_c$	$J''K''_aK''_c$	E''/ cm^{-1}	ω_{if}(calc.)/ cm^{-1}	ω_{if}(obs.)^a/ cm^{-1}	$\Delta\omega_{o-c}$/ cm^{-1}	$S(f-i)^b$/ D^2	$I_{\mathrm{Rel.}}(\omega)^c$
ν_3	3 2 2	4 1 3	515.930	2193.832	-	-	.338(-1)	.020
ν_2	3 3 0	3 3 1	458.283	2198.286	-	-	.179(-1)	.016
ν_3	3 0 3	4 1 4	403.529	2206.694	-	-	.667(-1)	.088
ν_2	2 2 0	2 2 1	218.620	2208.750	2208.417	-.333	.138(-1)	.032
ν_3	3 1 3	4 0 4	402.725	2215.386	-	-	.701(-1)	.031
ν_2	1 1 0	1 1 1	60.021	2218.744	2218.393	-.347	.912(-2)	.144
ν_3	2 0 2	3 1 3	253.969	2223.321	2223.706	.385	.576(-1)	.225
ν_2	3 2 1	3 2 2	354.677	2225.758	2225.501	-.257	.195(-1)	.012
ν_3	2 1 2	3 0 3	251.316	2239.296	2239.637	.341	.544(-1)	.073
ν_2	2 1 1	2 1 2	138.815	2240.803	2240.512	-.291	.108(-1)	.097
ν_3	2 2 1	3 1 2	326.011	2242.002	2242.303	.301	.134(-1)	.032
ν_3	4 1 4	4 2 3	531.158	2243.913	-	-	.789(-1)	.014
ν_3	1 0 1	2 1 2	138.815	2244.698	2245.109	.411	.490(-1)	.444
ν_2	1 0 1	0 0 0	0.000	2247.018	2246.697	-.321	.160(-2)	.013
ν_3	4 2 3	4 3 2	645.411	2248.461	-	-	.819(-1)	.019
ν_3	3 2 2	3 3 1	458.283	2251.479	-	-	.551(-1)	.050
ν_3	3 2 1	3 3 0	459.763	2257.003	2257.495	.492	.714(-1)	.065
ν_3	4 2 2	4 3 1	654.321	2260.854	-	-	.147(+0)	.033
ν_3	4 0 4	4 1 3	515.930	2260.857	2261.176	.321	.863(-1)	.052
ν_3	3 1 3	3 2 2	354.677	2263.434	2263.807	.477	.494(-1)	.032
ν_2	3 1 2	3 1 3	253.969	2266.476	-	-	.167(-1)	.067
ν_3	1 1 1	2 0 2	131.594	2270.761	2271.135	.374	.298(-1)	.096
ν_3	2 1 2	2 2 1	218.620	2271.991	2272.395	.404	.374(-1)	.064
ν_3	0 0 0	1 1 1	60.021	2274.965	2275.403	.438	.395(-1)	.638
ν_3	4 1 3	4 2 2	581.235	2278.538	2279.085	.547	.179(+0)	.023
ν_2	2 2 1	2 0 2	131.594	2284.166	2283.810	-.376	.902(-2)	.029
ν_3	3 0 3	3 1 2	326.011	2284.211	2284.565	.354	.907(-1)	.217
ν_2	4 1 3	4 1 4	403.529	2287.271	2287.118	-.153	.244(-1)	.033
ν_3	3 1 2	3 2 1	376.204	2287.456	-	-	.138(+0)	.077
ν_3	2 1 1	2 2 0	223.813	2288.152	2288.623	.471	.740(-1)	.123
ν_2	3 2 2	3 0 3	251.316	2288.329	-	-	.189(-1)	.026

Table 2 (*continued*).

Mode	$J'K_a'K_c'$	$J''K_a''K_c''$	E''/ cm^{-1}	ω_{if}(calc.)/ cm^{-1}	ω_{if}(obs.)^a/ cm^{-1}	$\Delta\omega_{o-c}$/ cm^{-1}	$S(f-i)^b$/ D^2	$I_{Rel.}(\omega)^c$
ν_2	5 1 5	4 1 4	403.529	2290.791	2290.658^e	-.133	.470(-2)	.006
ν_2	4 2 3	4 0 4	402.725	2295.736	-	-	.260(-1)	.012
ν_2	5 1 4	5 1 5	586.266	2300.739	-	-	.306(-1)	.011
ν_3	2 0 2	2 1 1	175.859	2301.431	2301.830	.399	.866(-1)	.615
ν_2	2 1 1	1 1 0	72.433	2307.185	-	-	.331(-2)	.050
ν_3	1 0 1	1 1 0	72.433	2311.080	2311.512	.422	.647(-1)	.971
ν_3	2 2 0	3 1 3	253.969	2315.134	-	-	.369(-2)	.015
ν_2	3 3 1	3 1 2	326.011	2325.692	-	-	.503(-2)	.012
ν_2	3 1 2	2 1 1	175.859	2344.586	-	-	.262(-2)	.019
ν_3	1 1 0	1 0 1	45.678	2363.173	-	-	.573(-1)	.355
ν_3	2 1 1	2 0 2	131.594	2380.370	2380.824	.454	.584(-1)	.197
ν_2	2 2 0	1 0 1	45.678	2381.692	2381.367	-.335	.364(-2)	.023
ν_3	3 2 1	3 1 2	326.011	2390.755	-	-	.748(-1)	.187
ν_3	2 2 0	2 1 1	175.859	2393.244	2393.633	.389	.450(-1)	.333
ν_3	4 2 2	4 1 3	515.930	2399.245	-	-	.790(-1)	.051
ν_3	1 1 1	0 0 0	0.000	2402.355	2402.795	.440	.421(-1)	.369
ν_3	3 1 2	3 0 3	251.316	2412.344	-	-	.422(-1)	.061
ν_3	2 0 2	1 1 1	60.021	2417.269	2417.734	.465	.337(-1)	.578
ν_3	2 2 1	2 1 2	138.815	2429.198	2429.647	.449	.262(-1)	.256
ν_3	3 3 0	3 2 1	376.204	2444.134	-	-	.335(-1)	.020
ν_3	2 1 2	1 0 1	45.678	2444.933	2445.348	.415	.640(-1)	.410
ν_3	3 1 2	2 2 1	218.620	2445.040	2445.606	.566	.149(-1)	.028
ν_2	3 2 1	3 0 2	131.594	2448.841	2448.627	-.214	.288(-2)	.010
ν_3	3 2 2	3 1 3	253.969	2455.793	-	-	.313(-1)	.135
ν_3	4 1 3	4 0 4	402.725	2457.048	-	-	.296(-1)	.015
ν_3	3 3 1	3 2 2	354.677	2465.686	2466.041	.355	.314(-1)	.022
ν_3	3 0 3	2 1 2	138.815	2471.408	2471.865	.457	.725(-1)	.721
ν_2	3 3 0	2 1 1	175.859	2480.710	-	-	.675(-2)	.052
ν_3	3 1 3	2 0 2	131.594	2486.518	2486.932	.414	.973(-1)	.342
ν_3	4 2 3	4 1 4	403.529	2490.344	2490.782	.438	.298(-1)	.045
ν_3	2 2 1	1 1 0	72.433	2495.580	2496.014	.434	.617(-1)	1.000
ν_3	4 1 3	3 2 2	354.677	2505.096	2505.693	.597	.380(-1)	.027

Mode	$J'K'_aK'_c$	$J''K''_aK''_c$	E''/ cm^{-1}	ω_{if}(calc.)/ cm^{-1}	ω_{if}(obs.)^a/ cm^{-1}	$\Delta\omega_{o-c}$/ cm^{-1}	$S(f-i)^b$/ D^2	$I_{\mathrm{Rel.}}(\omega)^c$
ν_3	2 2 0	1 1 1	60.021	2509.082	2509.541	.457	.490(-1)	.874
ν_2	3 3 1	2 1 2	138.815	2512.889	2512.598	-.391	.911(-2)	.092
ν_3	4 0 4	3 1 3	253.969	2522.818	2523.271	.453	.111(+0)	.491
ν_3	4 1 4	3 0 3	251.316	2523.755	2523.953	.198	.456(-1)	.069
ν_2	4 3 1	3 1 2	326.011	2527.505	-	-	.716(-2)	.019
ν_3	3 2 2	2 1 1	175.859	2533.903	2534.328	.425	.695(-1)	.543
ν_2	4 2 2	3 0 3	251.316	2537.054	2537.200	.146	.900(-1)	.137
ν_3	5 1 4	4 2 3	531.158	2563.030	-	-	.684(-1)	.014
ν_3	4 2 3	3 1 2	326.011	2567.861	2568.302	.441	.923(-1)	.248
ν_3	5 0 5	4 1 4	403.529	2571.114	2571.585	.471	.146(+0)	.226
ν_3	5 1 5	4 0 4	402.725	2572.303	2572.755	.452	.141(+0)	.073
ν_2	4 3 2	3 1 3	253.969	2576.899	-	-	.177(-1)	.080
ν_3	3 2 1	2 1 2	138.815	2577.951	2578.462	.511	.314(-1)	.326
ν_3	3 3 1	2 2 0	223.813	2596.550	2596.960	.410	.923(-1)	.175
ν_3	3 3 0	2 2 1	218.620	2601.718	2602.146	.428	.919(-1)	.180

R.M.S. deviation of calculated from experimental frequencies = 0.388cm^{-1}.
73 lines considered.

[a] Data from Reference 6.
[b] Powers of ten in brackets.
[c] Max. integrated absorption coefficient = 1.127 × 10^{18}(cm. sec^{-1} mole^{-1}).
[d] Data from Shy J.T., Farley J.W. and Wing W.H., 1981, *Phys. Rev. A.*, **24**, 1146.
[e] Reassigned from $5_{05} - 4_{04}$ on frequency grounds.
Calculated $5_{05} - 4_{04}$ occurs at 2291.522cm^{-1}, with similar relative intensity.

calculations puts this transition at 3169·055 cm^{-1}, almost exactly at the frequency obtained from adding the difference in experimental and calculated ν_1 to the experimentally measured line, thus confirming their reassignment on frequency grounds.

Nuclear spin considerations, on the other hand, predict that the *ortho*-$5_{15} - 4_{14}$ line ought to be three times as intense as its *para*-H_2D^+ neighbour. So far, this has not been reported. Given our error in the $5_{05} - 4_{04}$, we predict the $5_{15} - 4_{14}$ transition should occur at 3168·079 cm^{-1} and ought to be a candidate for observation.

In addition, our results indicate that one transition in each of the ν_2/ν_3 manifolds ought also to be reassigned. For H_2D^+, this is the line at 2290·658 cm^{-1} which we assign to ν_2 $5_{15} - 4_{14}$ (calculated frequency 2290·791 cm^{-1}) rather than ν_2 $5_{05} - 4_{04}$ (calculated frequency 2291·522 cm^{-1}). In this way, we get a value of $\Delta\omega_{o-c}$ of

Table 3. Calculated and observed ν_1 transitions for H_2D^+. Relative intensities calculated at 300 K.

$J'K'_aK'_c$	$J''K''_aK''_c$	E''/ cm^{-1}	ω_{if}(calc.)/ cm^{-1}	ω_{if}(obs.)^a/ cm^{-1}	$\Delta\omega_{o-c}$/ cm^{-1}	$S(f-i)^b$/ D^2	$I_{Rel.}(\omega)^c$
3 1 2	4 1 3	515.930	2801.434	-	-	.229(-1)	.165
4 1 4	5 1 5	586.266	2805.081	-	-	.248(-1)	.127
3 1 3	4 1 4	403.529	2839.880	2839.387	-.493	.206(-1)	.258
2 1 1	3 1 2	326.011	2841.480	2840.962	-.518	.175(-1)	.318
2 0 2	3 0 3	251.316	2872.393	2871.897	-.496	.167(-1)	.146
2 1 2	3 1 3	253.969	2875.302	2874.811	-.491	.157(-1)	.406
1 1 0	2 1 1	175.859	2887.870	2887.370	-.500	.102(-1)	.387
2 0 2	2 2 1	218.620	2905.089	2904.657	-.531	.196(-2)	.020
1 0 1	2 0 2	131.594	2907.020	2906.523	-.497	.121(-1)	.190
1 1 1	2 1 2	138.815	2912.112	2911.635	-.477	.937(-2)	.428
0 0 0	1 0 1	45.678	2947.284	2946.802	-.482	.664(-2)	.160
2 1 2	2 1 1	175.859	2953.412	2952.940	-.472	.626(-2)	.243
3 2 2	3 2 1	376.204	2963.958	2963.513	-.445	.136(-1)	.068
3 3 1	3 3 0	459.763	2975.422	2975.064	-.358	.335(-1)	.335
1 1 1	1 1 0	72.433	2978.494	2978.045	-.449	.105(-1)	.675
3 3 0	3 3 1	458.283	2978.843	2978.492	-.451	.328(-1)	.332
2 2 1	2 2 0	223.813	2980.403	2979.987	-.426	.213(-1)	.221
2 2 0	2 2 1	218.620	2991.562	2991.162	-.400	.203(-1)	.217
1 1 0	1 1 1	60.021	3003.708	3003.276	-.432	.974(-2)	.669
3 2 1	3 2 2	354.677	3009.510	3009.123	-.397	.114(-1)	.064
2 1 1	2 1 2	138.815	3028.677	3028.263	-.414	.497(-2)	.236
1 0 1	0 0 0	0.000	3038.614	3038.177	-.437	.696(-2)	.215
3 1 2	3 1 3	253.969	3063.396	3063.006	-.390	.332(-2)	.092
2 1 2	1 1 1	60.021	3069.250	3068.845	-.405	.111(-1)	.780
2 2 1	2 0 2	131.594	3072.622	3072.190	-.432	.953(-3)	.016
2 0 2	1 0 1	45.678	3078.031	3077.611	-.420	.136(-1)	.341
2 1 1	1 1 0	72.433	3095.059	3094.761	-.298	.104(-1)	.694
3 1 3	2 1 2	138.815	3104.594	3104.207	-.387	.205(-1)	1.000
3 0 3	2 0 2	131.594	3110.049	3109.645	-.404	.210(-1)	.353

Table 3 (*continued*).

$J'K'_aK'_c$	$J''K''_aK''_c$	E''/ cm^{-1}	ω_{if}(calc.)/ cm^{-1}	ω_{if}(obs.)^a/ cm^{-1}	$\Delta\omega_{o-c}$/ cm^{-1}	$S(f-i)^b$/ D^2	$I_{\mathrm{Rel.}}(\omega)^c$
3 2 2	2 2 1	218.620	3121.541	3121.202	-.339	.123(-1)	.137
4 1 4	3 1 3	253.969	3137.378	3137.007	-.371	.303(-1)	.859
4 0 4	3 0 3	251.316	3139.578	3139.197	-.381	.303(-1)	.290
3 2 1	2 2 0	223.813	3140.374	3140.044	-.330	.121(-1)	.132
3 1 2	2 1 1	175.859	3141.506	3141.131	-.375	.184(-1)	.760
4 2 3	3 2 2	354.677	3161.297	3160.971	-.326	.230(-1)	.135
4 3 2	3 3 1	458.283	3164.560	-	-	.134(-1)	.143
5 1 5	4 1 4	403.529	3168.432	-	-	.411(-1)	.574
5 0 5	4 0 4^d	402.725	3169.055	3168.702	-.353	.407(-1)	.190
4 3 1	3 3 0	459.763	3174.389	-	-	.130(-1)	.139
4 1 3	3 1 2	326.011	3179.336	3178.973	-.363	.257(-1)	.521
4 2 2	3 2 1	376.204	3194.284	3193.963	-.321	.225(-1)	.120
6 1 6	5 1 5	586.266	3198.416	-	-	.529(-1)	.310
6 0 6	5 0 5	586.049	3198.543	-	-	.530(-1)	.104
5 1 4	4 1 3	515.930	3208.535	3208.187	-.348	.339(-1)	.280
5 3 3	4 3 2	645.411	3208.582	-	-	.256(-1)	.113

R.M.S. deviation of calculated from experimental frequencies = $0.421\mathrm{cm}^{-1}$.
37 lines considered.

[a] Data from Reference 10.
[b] Powers of ten in brackets.
[c] Max. integrated absorption coefficient = 2.220×10^{17} (cm. sec^{-1} mole^{-1}).
[d] Reassigned by Kozin *et al* (Ref. 10) (see text).

$-0{\cdot}133\,\mathrm{cm}^{-1}$, in line with other nearby ν_2 lines. Using the original assignment would have given $\Delta\omega_{o-c} = -0{\cdot}864\,\mathrm{cm}^{-1}$, which is more than twice as large as any other value of $\Delta\omega_{o-c}$ found for ν_2.

We also consider the D_2H^+ ν_2 transition at $2040{\cdot}760\,\mathrm{cm}^{-1}$ ought to be reassigned from $6_{06} - 5_{15}$ (calculated frequency $2041{\cdot}641\,\mathrm{cm}^{-1}$) to $5_{15} - 4_{04}$ (calculated frequency $2040{\cdot}678\,\mathrm{cm}^{-1}$). Here again the value of $\Delta\omega_{o-c} = 0{\cdot}082\,\mathrm{cm}^{-1}$ is more typical of the trend we see than the $0{\cdot}881\,\mathrm{cm}^{-1}$ that would be obtained using the original assignment. As further support for this reassignment we can add that the $5_{15} - 4_{04}$ transition is calculated to be more than three times as intense as the $6_{06} - 5_{15}$ line.

Pure rotational transitions in the ground state are given for H_2D^+ and D_2H^+ in

Table 4. Calculated and observed ν_2 and ν_3 transitions for D_2H^+. Relative intensities calculated at 150 K.

Mode	$J'K'_aK'_c$	$J''K''_aK''_c$	E''/ cm^{-1}	ω_{if}(calc.)/ cm^{-1}	ω_{if}(obs.)^a/ cm^{-1}	$\Delta\omega_{o-c}$/ cm^{-1}	$S(f-i)^b$/ D^2	$I_{\mathrm{Rel.}}(\omega)^c$
ν_2	3 2 2	4 3 1	523.259	1712.856	-	-	.423(-1)	.010
ν_2	5 1 5	6 0 6	630.074	1726.226	-	-	.174(+0)	.015
ν_2	4 1 3	5 2 4	585.431	1754.103	-	-	.868(-1)	.012
ν_2	2 1 2	3 2 1	295.947	1766.755	-	-	.156(-1)	.017
ν_2	2 2 1	3 3 0	377.687	1767.693	-	-	.501(-1)	.025
ν_2	2 2 0	3 3 1	377.058	1772.250	-	-	.497(-1)	.051
ν_2	4 0 4	5 1 5	460.771	1772.445	-	-	.138(+0)	.063
ν_2	4 1 4	5 0 5	460.245	1773.975	-	-	.137(+0)	.032
ν_2	4 2 3	5 1 4	574.563	1782.237	1782.287^d	.050	.776(-1)	.006
ν_2	3 1 2	4 2 3	419.333	1786.040	1786.330^d	.290	.612(-1)	.021
ν_2	6 1 5	6 2 4	869.008	1807.295	1807.347^d	.052	.474(-1)	.000
ν_2	3 0 3	4 1 4	317.135	1816.129	1816.249	.120	.102(+0)	.095
ν_2	2 1 1	3 2 2	283.242	1816.290	-	-	.450(-1)	.116
ν_2	3 1 3	4 0 4	315.621	1820.670	-	-	.101(+0)	.191
ν_2	1 1 1	2 2 0	182.033	1831.786	1832.041^d	.255	.253(-1)	.173
ν_2	4 0 4	4 1 3	398.881	1834.335	-	-	.229(-1)	.020
ν_2	3 2 2	4 1 3	398.881	1837.233	1837.312^d	.079	.431(-1)	.037
ν_2	1 1 0	2 2 1	179.139	1847.558	1847.885	.327	.362(-1)	.129
ν_2	3 1 3	3 2 2	283.242	1853.049	1853.182^d	.133	.189(-1)	.050
ν_2	5 1 4	5 2 3	643.070	1854.082	1854.231^d	.149	.542(-1)	.002
ν_2	2 0 2	3 1 3	199.962	1854.841	1855.068	.227	.683(-1)	.399
ν_2	3 2 2	3 3 1	377.058	1859.057	-	-	.174(-1)	.019
ν_2	2 1 2	3 0 3	196.024	1866.678	1866.841^d	.163	.631(-1)	.193
ν_2	3 0 3	3 1 2	251.194	1882.070	1882.201^d	.131	.270(-1)	.049
ν_2	2 1 2	2 2 1	179.139	1883.564	1883.777	.213	.138(-1)	.050
ν_2	1 0 1	2 1 2	110.228	1887.982	1888.280^d	.298	.410(-1)	.289
ν_2	4 1 3	4 2 2	450.584	1888.951	-	-	.591(-1)	.032
ν_2	3 3 1	4 2 2	450.584	1889.173	-	-	.213(-1)	.011
ν_2	2 2 1	3 1 2	251.194	1894.186	1894.316	.130	.171(-1)	.031
ν_2	5 2 3	5 3 2	709.447	1895.478	1895.431^d	-.057	.456(-1)	.001
ν_2	3 1 2	3 2 1	295.947	1909.426	-	-	.504(-1)	.060

Table 4 (*continued*).

Mode	$J'K'_aK'_c$	$J''K''_aK''_c$	E''/ cm^{-1}	ω_{if}(calc.)/ cm^{-1}	ω_{if}(obs.)[a]/ cm^{-1}	$\Delta\omega_{o-c}$/ cm^{-1}	$S(f-i)$[b]/ D^2	$I_{\mathrm{Rel.}}(\omega)$[c]
ν_2	1 1 1	2 0 2	101.675	1912.145	1912.387[d]	.242	.269(-1)	.416
ν_3	4 1 4	4 3 1	523.259	1916.736	1916.451[d]	-.285	.170(-1)	.005
ν_2	2 1 1	2 2 0	182.033	1917.499	1917.857[d]	.358	.273(-1)	.196
ν_2	2 0 2	2 1 1	136.311	1918.492	1918.732	.240	.323(-1)	.359
ν_2	0 0 0	1 1 1	49.247	1918.578	1918.908	.330	.235(-1)	.604
ν_3	4 1 3	5 1 4	574.563	1934.405	1933.801[d]	-.604	.785(-2)	.001
ν_3	1 0 1	2 2 0	182.033	1937.260	-	-	.278(-2)	.020
ν_2	1 0 1	1 1 0	57.976	1940.234	1940.551	.317	.288(-1)	.344
ν_2	2 2 0	3 1 3	199.962	1949.346	1949.533	.183	.375(-2)	.023
ν_3	3 1 2	4 1 3	398.881	1952.584	1951.920[d]	-.664	.100(-1)	.009
ν_3	2 2 0	3 2 1	295.947	1962.349	-	-	.117(-1)	.014
ν_3	2 2 1	3 2 2	283.242	1972.132	1971.355	-.777	.872(-2)	.024
ν_3	2 1 1	3 1 2	251.194	1974.566	1973.852	-.714	.116(-1)	.022
ν_2	1 1 0	1 0 1	34.902	1991.795	1992.130	.335	.345(-1)	.527
ν_2	4 2 2	4 1 3	398.881	1995.340	1995.508	.168	.101(+0)	.095
ν_2	2 1 1	2 0 2	101.675	1997.858	1998.203	.345	.446(-1)	.720
ν_3	2 0 2	3 0 3	196.024	1998.636	1997.962	-.674	.657(-2)	.022
ν_3	1 1 0	2 1 1	136.311	2000.689	1999.879	-.710	.116(-1)	.135
ν_2	3 2 1	3 1 2	251.194	2001.543	2001.744	.201	.826(-1)	.159
ν_3	2 1 2	3 1 3	199.962	2003.344	2002.750	-.594	.476(-2)	.030
ν_2	2 0 2	1 1 1	49.247	2005.556	2005.844	.288	.121(-1)	.324
ν_3	4 0 4	4 2 3	419.333	2006.574	-	-	.337(-1)	.013
ν_2	3 1 2	3 0 3	196.024	2009.349	2009.696	.347	.444(-1)	.146
ν_2	2 2 0	2 1 1	136.311	2012.997	2013.196	.199	.467(-1)	.545
ν_2	1 1 1	0 0 0	0.000	2013.819	2014.106	.287	.169(-1)	.729
ν_2	4 3 1	4 2 2	450.584	2014.506	2014.433	-.073	.904(-1)	.052
ν_3	3 0 3	3 2 2	283.242	2014.795	2014.263	-.532	.179(-1)	.051
ν_3	2 0 2	2 2 1	179.139	2015.522	-	-	.476(-2)	.019
ν_3	1 0 1	2 0 2	101.675	2017.619	-	-	.897(-2)	.146
ν_3	1 1 1	2 1 2	110.228	2019.202	2018.437	-.765	.705(-2)	.053

Table 4 (*continued*).

Mode	$J'K'_aK'_c$	$J''K''_aK''_c$	E''/ cm^{-1}	ω_{if}(calc.)/ cm^{-1}	ω_{if}(obs.)^a/ cm^{-1}	$\Delta\omega_{o-c}$/ cm^{-1}	$S(f-i)^b$/ D^2	$I_{\mathrm{Rel.}}(\omega)^c$
ν_2	3 0 3	2 1 2	110.228	2023.036	2023.243	.207	.215(-1)	.162
ν_2	4 1 3	4 0 4	315.621	2023.913	2024.230	.317	.423(-1)	.089
ν_2	3 1 2	2 2 1	179.139	2026.234	2026.631	.397	.498(-2)	.019
ν_2	2 1 2	1 0 1	34.902	2027.800	2028.024	.224	.192(-1)	.299
ν_2	4 0 4	3 1 3	199.962	2033.255	2033.393	.138	.277(-1)	.178
ν_2	3 1 3	2 0 2	101.675	2034.617	2034.780	.163	.229(-1)	.377
ν_2	2 2 1	2 1 2	110.228	2035.152	2035.359	.207	.245(-1)	.186
ν_2	3 2 2	3 1 3	199.962	2036.153	2036.333	.180	.339(-1)	.218
ν_2	5 1 4	5 0 5	460.245	2036.908	-	-	.419(-1)	.011
ν_2	4 1 4	3 0 3	196.024	2038.196	2038.310	.114	.276(-1)	.092
ν_2	3 3 0	3 2 1	295.947	2038.807	2038.936	.129	.565(-1)	.072
ν_2	5 0 5	4 1 4	317.135	2038.848	2038.634	-.214	.324(-1)	.034
ν_2	4 2 3	4 1 4	317.135	2039.665	2039.834	.169	.384(-1)	.040
ν_2	5 1 5	4 0 4	315.621	2040.678	2040.760^e	.082	.322(-1)	.068
ν_2	6 0 6	5 1 5	460.771	2041.641	-	-	.367(-1)	.019
ν_3	0 0 0	1 0 1	34.902	2044.310	2043.515	-.795	.814(-2)	.128
ν_2	5 2 4	5 1 5	460.771	2044.455	-	-	.406(-1)	.021
ν_2	4 4 0	4 3 1	523.259	2051.320	-	-	.646(-1)	.019
ν_2	4 3 2	4 2 3	419.333	2052.536	-	-	.373(-1)	.015
ν_2	4 1 3	3 2 2	283.242	2056.292	-	-	.119(-1)	.035
ν_2	3 3 1	3 2 2	283.242	2056.514	2056.416	-.098	.352(-1)	.103
ν_3	2 1 2	2 1 1	136.311	2066.995	2066.415	-.580	.408(-2)	.049
ν_3	3 3 1	3 3 0	377.687	2069.161	2068.461	-.700	.469(-1)	.028
ν_3	3 3 0	3 3 1	377.058	2070.570	2069.869	-.701	.456(-1)	.054
ν_3	1 1 1	1 1 0	57.976	2071.454	2070.708	-.746	.181(-1)	.230
ν_3	2 2 1	2 2 0	182.033	2073.341	2072.607	-.734	.321(-1)	.249
ν_3	2 2 0	2 2 1	179.139	2079.157	2078.419	-.732	.284(-1)	.114
ν_2	2 2 1	1 1 0	57.976	2087.404	2087.630	.226	.199(-1)	.255
ν_3	1 1 0	1 1 1	49.247	2087.752	2086.990	-.762	.128(-1)	.357
ν_2	3 2 2	2 1 1	136.311	2099.804	2099.998	.194	.163(-1)	.199

Table 4 (*continued*).

Mode	$J'K'_aK'_c$	$J''K''_aK''_c$	E''/ cm^{-1}	ω_{if}(calc.)/ cm^{-1}	ω_{if}(obs.)^a/ cm^{-1}	$\Delta\omega_{o-c}$/ cm^{-1}	$S(f-i)^b$/ D^2	$I_{\text{Rel.}}(\omega)^c$
ν_2	2 2 0	1 1 1	49.247	2100.060	2100.307	.247	.106(-1)	.296
ν_2	4 2 3	3 1 2	251.194	2105.606	-	-	.166(-1)	.034
ν_2	5 2 4	4 1 3	398.881	2106.345	2106.301	-.044	.192(-1)	.019
ν_3	2 1 1	2 1 2	110.228	2115.532	2114.895	-.637	.185(-2)	.015
ν_3	1 0 1	0 0 0	0.000	2119.293	2118.588	-.705	.143(-1)	.652
ν_3	2 1 2	1 1 1	49.247	2154.058	2153.525	-.533	.347(-1)	1.000
ν_2	3 3 0	2 2 1	179.139	2155.615	-	-	.638(-2)	.027
ν_2	3 3 1	2 2 0	182.033	2157.723	2157.667	-.056	.135(-1)	.109
ν_3	2 0 2	1 0 1	34.902	2159.758	2159.145	-.613	.313(-1)	.519
ν_3	2 1 1	1 1 0	57.976	2167.785	2167.166	-.619	.269(-1)	.359
ν_2	4 3 2	3 2 1	295.947	2175.922	-	-	.118(-1)	.016
ν_2	4 2 2	3 1 3	199.962	2194.260	-	-	.233(-2)	.016
ν_3	3 0 3	2 0 2	101.675	2196.362	2195.861	-.501	.466(-1)	.829
ν_3	3 1 3	2 1 2	110.228	2196.871	2196.475	-.396	.590(-1)	.483
ν_3	3 2 2	2 2 1	179.139	2210.537	2210.331	-.206	.617(-1)	.262
ν_3	3 1 2	2 1 1	136.311	2215.154	2214.605	-.549	.449(-1)	.577
ν_3	3 2 1	2 2 0	182.033	2215.762	2215.437	-.235	.543(-1)	.450
ν_3	4 0 4	3 0 3	196.024	2229.883	-	-	.591(-1)	.216
ν_2	3 3 1	2 0 2	101.675	2238.082	2238.014	-.068	.582(-2)	.105
ν_3	4 1 4	3 1 3	199.962	2240.033	2239.809	-.224	.770(-1)	.544
ν_2	5 2 3	4 1 4	317.135	2247.925	2248.033	.108	.271(-1)	.031
ν_3	4 1 3	3 1 2	251.194	2257.774	2257.293	-.481	.594(-1)	.129
ν_3	4 2 3	3 2 2	283.242	2258.160	2257.968	-.192	.788(-1)	.252
ν_3	5 0 5	4 0 4	315.621	2264.103	2263.828	-.275	.756(-1)	.178
ν_3	4 2 2	3 2 1	295.947	2268.096	2267.719	-.377	.670(-1)	.095
ν_2	4 3 2	3 0 3	196.024	2275.846	-	-	.170(-1)	.063
ν_2	4 4 0	3 3 1	377.058	2279.011	2279.090	.079	.890(-1)	.117
ν_2	4 4 1	3 3 0	377.687	2279.461	2279.521	.060	.882(-1)	.058
ν_2	5 2 3	4 1 4	317.135	2287.790	-	-	.739(-1)	.087

Table 4 (*continued*).

Mode	$J'K'_aK'_c$	$J''K''_aK''_c$	E''/ cm^{-1}	ω_{if}(calc.)/ cm^{-1}	ω_{if}(obs.)^a/ cm^{-1}	$\Delta\omega_{o-c}$/ cm^{-1}	$S(f-i)^b$/ D^2	$I_{Rel.}(\omega)^c$
ν_3	5 1 4	4 1 3	398.881	2291.259	2290.873	-.386	.651(-1)	.070
ν_3	6 1 6	5 1 5	460.771	2293.824	-	-	.751(-1)	.045
ν_3	6 0 6	5 0 5	460.245	2299.322	-	-	.964(-1)	.029

R.M.S. deviation of calculated from experimental frequencies = 0.400cm^{-1}.
86 lines considered.

[a] Data from Reference 9.
[b] Powers of ten in brackets.
[c] Max. integrated absorption coefficient= 5.209 × 10^{17} (cm. sec^{-1} mole^{-1}).
[d] Data from Shy J.-T., 1982, *PhD. Dissertation*, Univ. of Arizona.
[e] Reassigned from $6_{06} - 5_{15}$ on frequency considerations.

Table 5. Calculated and observed v_1 transitions for D_2H^+. Relative intensities calculated at 300 K.

$J'K'_aK'_c$	$J''K''_aK''_c$	E''/ cm^{-1}	ω_{if}(calc.)/ cm^{-1}	ω_{if}(obs.)^a/ cm^{-1}	$\Delta\omega_{o-c}$/ cm^{-1}	$S(f-i)^b$/ D^2	$I_{Rel.}(\omega)^c$
1 1 1	2 2 0	182.033	2603.612	-	-	.173(-1)	.338
3 0 3	4 1 4	317.135	2613.922	-	-	.423(-1)	.218
1 1 0	2 2 1	179.139	2615.121	-	-	.223(-1)	.223
3 2 2	4 1 3	398.881	2617.148	-	-	.144(-1)	.101
3 1 3	4 0 4	315.621	2619.165	-	-	.408(-1)	.424
2 0 2	3 1 3	199.962	2637.868	2637.524	-.344	.304(-1)	.555
3 2 2	3 3 1	377.058	2638.972	-	-	.167(-1)	.130
2 1 2	3 0 3	196.024	2649.976	-	-	.262(-1)	.245
4 0 4	4 1 3	398.881	2650.396	-	-	.248(-1)	.175
3 1 3	3 2 2	283.242	2651.544	-	-	.189(-1)	.232
4 2 2	4 3 1	523.259	2658.453	-	-	.376(-1)	.147
1 0 1	2 1 2	110.228	2661.599	2661.258	-.341	.210(-1)	.296
2 1 2	2 2 1	179.139	2666.861	-	-	.125(-1)	.127
3 0 3	3 1 2	251.194	2679.863	-	-	.266(-1)	.193
4 1 3	4 2 2	450.584	2680.599	-	-	.519(-1)	.289
1 1 1	2 0 2	101.675	2683.971	2683.613	-.358	.116(-1)	.345
0 0 0	1 1 1	49.247	2688.055	-	-	.141(-1)	.542

Table 5 (*continued*).

$J'K'_aK'_c$	$J''K''_aK''_c$	E''/ cm^{-1}	ω_{if}(calc.)/ cm^{-1}	ω_{if}(obs.)^a/ cm^{-1}	$\Delta\omega_{o-c}$/ cm^{-1}	$S(f-i)^b$/ D^2	$I_{Rel.}(\omega)^c$
3 1 2	3 2 1	295.947	2689.345	-	-	.403(-1)	.237
2 1 1	2 2 0	182.033	2689.701	-	-	.210(-1)	.425
2 0 2	2 1 1	136.311	2701.519	2701.189	-.330	.274(-1)	.694
1 0 1	1 1 0	57.976	2713.851	-	-	.215(-1)	.398
1 1 0	1 0 1	34.902	2759.357	2759.036	-.321	.203(-1)	.427
2 1 1	2 0 2	101.675	2770.059	2769.753	-.306	.253(-1)	.776
3 2 1	3 1 2	251.194	2777.509	2777.196	-.313	.366(-1)	.275
2 2 0	2 1 1	136.311	2779.565	2779.238	-.327	.189(-1)	.493
4 2 2	4 1 3	398.881	2782.831	2782.543	-.288	.466(-1)	.345
1 1 1	0 0 0	0.000	2785.646	2785.332	-.314	.138(-1)	.693
2 0 2	1 1 1	49.247	2788.582	2788.300	-.282	.124(-1)	.494
3 1 2	3 0 3	196.024	2789.269	2788.990	-.279	.235(-1)	.231
4 3 1	4 2 2	450.584	2801.211	-	-	.322(-1)	.188
2 2 1	2 1 2	110.228	2802.746	2802.436	-.310	.106(-1)	.158
2 1 2	1 0 1	34.902	2811.098	2810.800	-.298	.211(-1)	.453
4 1 3	4 0 4	315.621	2815.561	2815.314	-.247	.206(-1)	.230
3 2 2	3 1 3	199.962	2816.068	2815.778	-.290	.155(-1)	.301
3 0 3	2 1 2	110.228	2820.829	2820.564	-.265	.284(-1)	.426
3 3 1	3 2 2	283.242	2823.574	-	-	.134(-1)	.175
3 1 3	2 0 2	101.675	2833.112	2832.828	-.284	.319(-1)	1.000
4 1 3	3 2 2	283.242	2847.940	-	-	.162(-1)	.214
4 0 4	3 1 3	199.962	2849.316	2849.066	-.250	.452(-1)	.889
5 2 4	5 1 5	460.771	2854.254	-	-	.179(-1)	.101
4 1 4	3 0 3	196.024	2854.682	2854.421	-.261	.461(-1)	.463
2 2 1	1 1 0	57.976	2854.998	2854.707	-.291	.201(-1)	.392
2 2 0	1 1 1	49.247	2866.628	2866.350	-.278	.150(-1)	.612
5 0 5	4 1 4	317.135	2875.177	2874.948	-.229	.618(-1)	.350
5 1 5	4 0 4	315.621	2877.189	2876.954	-.235	.620(-1)	.708
3 2 2	2 1 1	136.311	2879.719	2879.442	-.277	.229(-1)	.620

Table 5 (*continued*).

$J'K'_aK'_c$	$J''K''_aK''_c$	E''/ cm^{-1}	ω_{if}(calc.)/ cm^{-1}	ω_{if}(obs.)^a/ cm^{-1}	$\Delta\omega_{o-c}$/ cm^{-1}	$S(f-i)^b$/ D^2	$I_{\mathrm{Rel.}}(\omega)^c$
5 1 4	4 2 3	419.333	2885.351	-	-	.318(-1)	.111
4 2 3	3 1 2	251.194	2899.505	2899.242	-.263	.287(-1)	.225
6 0 6	5 1 5	460.771	2899.569	2899.362	-.207	.786(-1)	.451
6 1 6	5 0 5	460.245	2900.267	-	-	.787(-1)	.226
5 2 4	4 1 3	398.881	2916.143	2915.899	-.244	.384(-1)	.298
6 1 5	5 2 4	585.431	2917.023	-	-	.498(-1)	.158
3 2 1	2 1 2	110.228	2918.476	2918.238	-.238	.937(-2)	.145
7 0 7	6 1 6	630.248	2923.123	-	-	.960(-1)	.123
7 1 7	6 0 6	630.074	2923.384	-	-	.959(-1)	.246
3 3 1	2 2 0	182.033	2924.783	2924.524	-.249	.307(-1)	.676
3 3 0	2 2 1	179.139	2928.319	2928.067	-.252	.297(-1)	.332
8 0 8	7 1 7	825.162	2946.134	-	-	.114(+0)	.115
4 3 2	3 2 1	295.947	2951.777	2951.532	-.245	.299(-1)	.193
4 3 1	3 2 2	283.242	2968.552	2968.334	-.218	.252(-1)	.346
5 3 3	4 2 2	450.584	2972.063	-	-	.315(-1)	.194
4 2 2	3 1 3	199.962	2981.751	-	-	.534(-2)	.110
4 4 1	3 3 0	377.687	2989.625	-	-	.429(-1)	.189
4 4 0	3 3 1	377.058	2990.367	2990.154^d	-.213	.428(-1)	.378

R.M.S. deviation of calculated from experimental frequencies = 0.281cm^{-1}.
34 lines considered.

[a] Data from Reference 10.
[b] Powers of ten in brackets.
[c] Max. integrated absorption coefficient= 2.465×10^{17} (cm. sec^{-1} mole^{-1}).
[d] Reassigned from $4_{41} - 3_{30}$.

tables 6 and 7 respectively. We have considered the spectral range from 0 to 1500 cm^{-1}, and have included all transitions which have relative intensity of 0·1 or more at 300 K. In practice this reduces the range to a maximum ω_{if} of around 400 cm^{-1} for both molecules, and excludes all states with $J'' > 7$. It is our intention to perform a systematic study of transitions involving highly excited J states which would be appropriate for spectra recorded at higher temperatures.

Within these limits we find 32 transitions for H_2D^+ (table 6) and 42 for D_2H^+ (table 7). In table 6, we have also included the three experimentally observed lines

Table 6. Pure rotational transitions for H_2D^+ in the ground state. Relative intensities calculated at 300 K.

$J'K'_aK'_c$	$J''K''_aK''_c$	$E'/$ cm^{-1}	$E''/$ cm^{-1}	$\omega_{if}/$ cm^{-1}	$S(f-i)^a/$ D^2	$I_{Rel.}(\omega)^b$	$A^a_{if}/$ s^{-1}
2 2 0	2 2 1	223.813	218.620	5.193[c]	.127(+1)	.001	.112(-4)
1 1 0	1 1 1	72.433	60.021	12.412[d]	.606(+0)	.014	.121(-3)
1 0 1	0 0 0	45.678	0.000	45.678[e]	.405(+0)	.035	.121(-1)
2 1 2	1 1 1	138.815	60.021	78.794	.610(+0)	.328	.187(-1)
2 0 2	1 0 1	131.594	45.678	85.916	.761(+0)	.171	.302(-1)
2 1 1	1 1 0	175.859	72.433	103.426	.609(+0)	.503	.402(-1)
3 1 3	2 1 2	253.969	138.815	115.154	.107(+1)	.776	.702(-1)
3 0 3	2 0 2	251.316	131.594	119.722	.111(+1)	.297	.851(-1)
3 2 2	2 2 1	354.677	218.620	136.057	.688(+0)	.152	.777(-1)
4 1 4	3 1 3	403.529	253.969	149.560	.149(+1)	.974	.173(+0)
3 1 2	2 1 1	326.011	175.859	150.153	.104(+1)	1.000	.159(+0)
4 0 4	3 0 3	402.725	251.316	151.410	.149(+1)	.337	.181(+0)
3 2 1	2 2 0	376.204	223.813	152.391	.707(+0)	.184	.112(+0)
4 2 3	3 2 2	531.158	354.677	176.480	.121(+1)	.215	.232(+0)
5 1 5	4 1 4	586.266	403.529	182.737	.190(+1)	.844	.330(+0)
5 0 5	4 0 4	586.049	402.725	183.324	.190(+1)	.284	.333(+0)
4 3 2	3 3 1	645.411	458.283	187.129	.752(+0)	.268	.171(+0)
4 1 3	3 1 2	515.930	326.011	189.919	.139(+1)	.955	.331(+0)
4 3 1	3 3 0	654.321	459.763	194.558	.754(+0)	.284	.193(+0)
4 2 2	3 2 1	581.235	376.204	205.032	.126(+1)	.256	.378(+0)
5 2 4	4 2 3	744.825	531.158	213.668	.166(+1)	.172	.462(+0)
6 1 6	5 1 5	801.484	586.266	215.217	.230(+1)	.555	.554(+0)
6 0 6	5 0 5	801.430	586.049	215.381	.230(+1)	.185	.555(+0)
5 1 4	4 1 3	738.472	515.930	222.541	.171(+1)	.609	.538(+0)
5 3 3	4 3 2	876.291	645.411	230.879	.135(+1)	.272	.473(+0)
7 1 7	6 1 6	1048.709	801.484	247.225	.271(+1)	.288	.860(+0)
5 3 2	4 3 1	903.750	654.321	249.429	.137(+1)	.300	.607(+0)
5 2 3	4 2 2	832.870	581.235	251.635	.169(+1)	.177	.789(+0)
6 1 5	5 1 4	990.739	738.472	252.267	.208(+1)	.309	.808(+0)
6 3 4	5 3 3	1147.516	876.291	271.226	.185(+1)	.158	.892(+0)

Table 6 (*continued*).

$J'K'_aK'_c$	$J''K''_aK''_c$	$E'/$ cm^{-1}	$E''/$ cm^{-1}	$\omega_{if}/$ cm^{-1}	$S(f-i)^a/$ D^2	$I_{\mathrm{Rel.}}(\omega)^b$	$A^a_{if}/$ s^{-1}
8 1 8	7 1 7	1327.521	1048.709	278.812	.312(+1)	.122	.125(+1)
7 1 6	6 1 5	1272.962	990.739	282.224	.248(+1)	.130	.117(+1)
6 3 3	5 3 2	1205.599	903.750	301.850	.191(+1)	.167	.127(+1)
4 3 1	3 1 2	654.321	326.011	328.310	.971(-1)	.153	.120(+0)
5 3 2	4 1 3	903.750	515.930	387.819	.131(+0)	.104	.217(+0)

[a] Powers of ten in brackets.

[b] Max. integrated absorption coefficient = 2.343 × 10^{17} (cm. sec^{-1} mole^{-1}).

[c] Observed at 5.202cm^{-1}(Ref. 14).

[d] Observed at 12.423cm^{-1}(Ref. 13).

[e] Observed at 45.703cm^{-1}(Ref. 16).

Table 7. Pure rotational transitions for D_2H^+ in the ground state. Relative intensities calculated at 300 K.

$J'K'_aK'_c$	$J''K''_aK''_c$	$E'/$ cm^{-1}	$E''/$ cm^{-1}	$\omega_{if}/$ cm^{-1}	$S(f-i)^a/$ D^2	$I_{\mathrm{Rel.}}(\omega)^b$	$A^a_{if}/$ s^{-1}
2 2 0	2 1 1	182.033	136.311	45.723[c]	.380(+0)	.057	.228(-2)
2 1 2	1 0 1	110.228	34.902	75.326	.394(+0)	.122	.106(-1)
3 2 2	3 1 3	283.242	199.962	83.280	.329(+0)	.111	.853(-2)
3 0 3	2 1 2	196.024	110.228	85.796	.515(+0)	.140	.146(-1)
3 1 3	2 0 2	199.962	101.675	98.287	.581(+0)	.421	.247(-1)
4 1 3	3 2 2	398.881	283.242	115.639	.292(+0)	.118	.158(-1)
4 0 4	3 1 3	315.621	199.962	115.660	.804(+0)	.485	.433(-1)
4 1 4	3 0 3	317.135	196.024	121.111	.821(+0)	.273	.509(-1)
2 2 1	1 1 0	179.139	57.976	121.163	.398(+0)	.257	.444(-1)
2 2 0	1 1 1	182.033	49.247	132.786	.303(+0)	.478	.446(-1)
5 0 5	4 1 4	460.245	317.135	143.109	.108(+1)	.267	.901(-1)
5 1 5	4 0 4	460.771	315.621	145.150	.108(+1)	.554	.945(-1)
3 2 2	2 1 1	283.242	136.311	146.931	.437(+0)	.540	.621(-1)
4 2 3	3 1 2	419.333	251.194	168.139	.526(+0)	.234	.871(-1)
6 0 6	5 1 5	630.074	460.771	169.302	.134(+1)	.443	.158(+0)

Table 7 (*continued*).

$J'K'_aK'_c$	$J''K''_aK''_c$	E'/ cm^{-1}	E''/ cm^{-1}	ω_{if}/ cm^{-1}	$S(f-i)^a$/ D^2	$I_{\mathrm{Rel.}}(\omega)^b$	A^a_{if}/ s^{-1}
6 1 6	5 0 5	630.248	460.245	170.003	.134(+1)	.224	.159(+0)
3 2 1	2 1 2	295.947	110.228	185.719	.189(+0)	.195	.544(-1)
5 2 4	4 1 3	585.431	398.881	186.550	.678(+0)	.353	.125(+0)
6 1 5	5 2 4	774.691	585.431	189.260	.858(+0)	.187	.140(+0)
7 0 7	6 1 6	825.105	630.248	194.858	.160(+1)	.148	.248(+0)
3 3 1	2 2 0	377.058	182.033	195.025	.633(+0)	1.000	.210(+0)
7 1 7	6 0 6	825.162	630.074	195.088	.160(+1)	.296	.249(+0)
3 1 2	2 2 1	377.687	179.139	198.548	.618(+0)	.509	.217(+0)
6 2 5	5 1 4	779.613	574.563	205.049	.895(+0)	.117	.186(+0)
8 0 8	7 1 7	1045.179	825.162	220.018	.186(+1)	.163	.366(+0)
4 3 2	3 2 1	519.237	295.947	223.290	.586(+0)	.332	.228(+0)
7 2 6	6 1 5	1000.320	774.691	225.628	.115(+1)	.133	.276(+0)
4 3 1	3 2 2	523.259	283.242	240.017	.507(+0)	.683	.244(+0)
5 3 3	4 2 2	695.841	450.584	245.257	.580(+0)	.362	.245(+0)
4 2 2	3 1 3	450.584	199.962	250.622	.108(+0)	.233	.594(-1)
4 4 1	3 3 0	643.244	377.687	265.557	.921(+0)	.460	.601(+0)
4 4 0	3 3 1	643.353	377.058	266.295	.920(+0)	.925	.606(+0)
5 3 2	4 2 3	709.447	419.333	290.114	.366(+0)	.171	.255(+0)
5 4 2	4 3 1	820.269	523.259	297.010	.838(+0)	.491	.626(+0)
5 4 1	4 3 2	821.184	519.237	301.947	.826(+0)	.252	.648(+0)
6 4 3	5 3 2	1032.584	709.447	323.137	.762(+0)	.103	.621(+0)
5 5 1	4 4 0	976.179	643.353	332.826	.124(+1)	.479	.130(+1)
5 5 0	4 4 1	976.196	643.244	332.952	.124(+1)	.240	.130(+1)
6 4 2	5 3 3	1036.658	695.841	340.817	.706(+0)	.220	.675(+0)
6 3 3	5 2 4	936.779	585.431	351.348	.238(+0)	.131	.249(+0)
6 5 2	5 4 1	1186.132	821.184	364.947	.114(+1)	.107	.133(+1)
6 5 1	5 4 2	1186.302	820.269	366.034	.114(+1)	.215	.135(+1)
6 6 0	5 5 1	1373.390	976.179	397.211	.158(+1)	.158	.239(+1)

[a] Powers of ten in brackets.

[b] Max. integrated absorption coefficient = 1.392 × 10^{17} (cm. sec^{-1} mole^{-1}).

[c] Observed at 45.702cm^{-1}(Ref. 16).

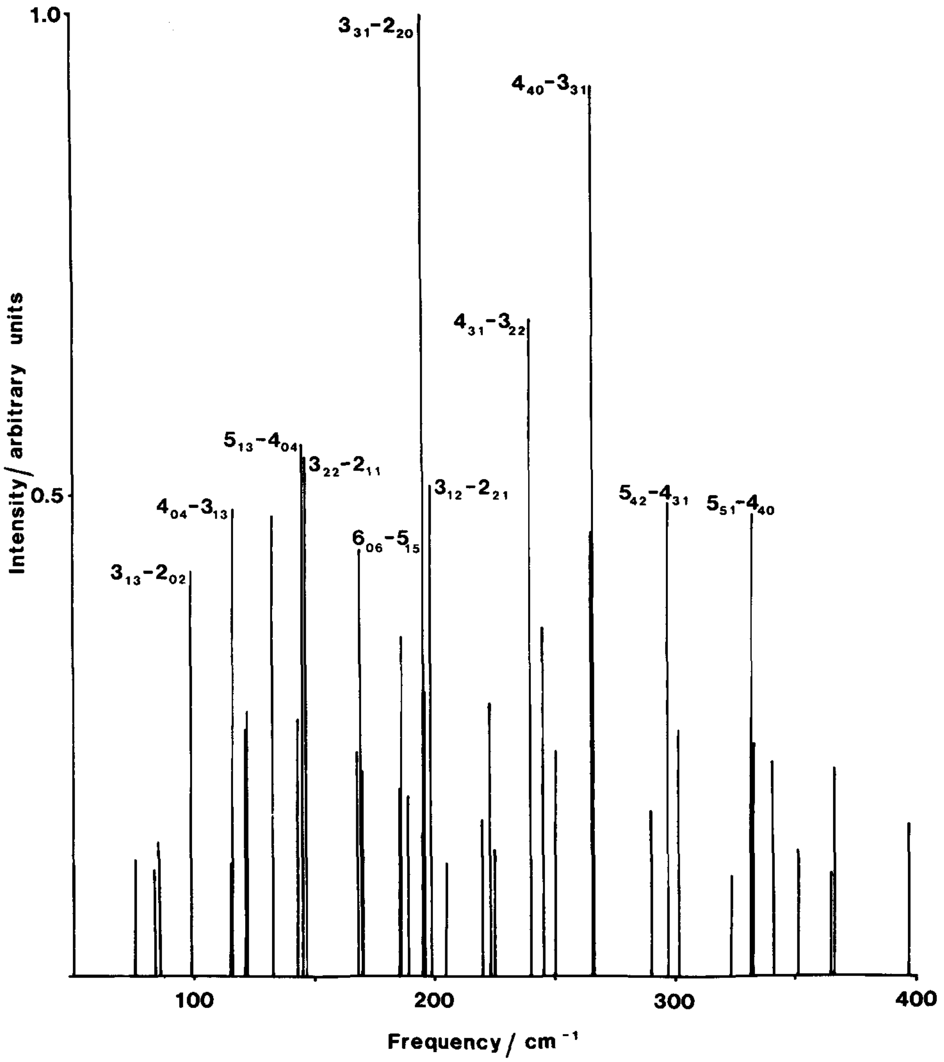

Figure. Rotational spectrum of D_2H^+ at 300 K.

[13–15], even though their relative intensities at this temperature fall below the 10 per cent cut-off. The calculated frequencies are in very good agreement with experiment. We obtain values of 5·193 cm^{-1} for the $2_{20}-2_{21}$ line measured at 5·202 cm^{-1} [14] and 12·412 cm^{-1} for the $1_{10}-1_{11}$ line at 12.423 cm^{-1} [13].

Recently, Evenson [16], has measured the $1_{01}-0_{00}$ line at 45·703 cm^{-1}, again in good agreement with our calculated value of 45·678 cm^{-1}. In addition, he was able to identify a line at 45·702 cm^{-1} as the $2_{20}-2_{11}$ line of D_2H^+, is the first measured line for this species, using data prepared for this paper (predicted frequency 45·723 cm^{-1}).

These results bear out the trend of our ro-vibrational data, which indicated that the rotational term values were being computed with a high level of accuracy and that the deviation from experiment was due to errors in the vibrational band origin.

The simulated rotational spectrum of D_2H^+ is presented in the figure. At the assumed temperature of 300 K it is clear that there are a large number of intense transitions that may be observable.

5. Conclusions

Computer calculations based on the theory developed above have produced a representation of the rotational and ro-vibrational transitions of H_2D^+ and D_2H^+ which accords very well the available experimental data. The small, systematic deviations from experiment observed in the ro-vibrational calculations are almost totally accounted for by the errors in the vibrational band origins.

In addition to comparing calculated frequencies with those measured, we have predicted a number of lines which ought to be observable on the basis of relative intensity considerations. Near exact experimental frequencies should be given by correcting the calculations for the error in the vibrational fundamental of interest.

We have also made three reassignments of the experimental data on frequency considerations, which we hope will be of assistance in fitting accurate spectroscopic constants to the measured lines.

There is currently considerable interest in rectifying the dearth of data on the pure rotational transitions of H_2D^+ and D_2H^+. Our calculations give excellent agreement with what experimental information is available, and we hope that the predictions contained in this paper will be of assistance to those experimentalists working in this area.

Finally, for reasons of space we have limited ourselves considerably in the amount of data presented in this paper. As well as different rotational and ro-vibrational manifolds already mentioned, we can calculate relative intensities at any temperature which may be of interest. Additional information will be supplied by the authors on request.

We would like to acknowledge the considerable assistance provided by Dr. Per Jensen in allowing us access to his unpublished ro-vibrational line strengths and transitions for H_2D^+ and H_3^+. The United Kingdom SERC is also thanked for financial support for one of us (S.M.) and for providing computing facilities.

References

[1] Oka, T., 1980, *Phys. Rev. Lett.*, **45**, 531.

[2] Shy, J.-T., Farley, J. W., Lamb, W. E. Jnr., and Wing, W. H., 1980, *Phys. Rev. Lett.*, **45**, 535.

[3] Watson, J. K. G., Foster, S. C., McKeller, A. R. W., Bernath, P., Amano, T., Pan, F.-S., Crofton, M. W., Altmann, R. S., and Oka, T., 1984, *Can. J. Phys.*, **62**, 1875.

[4] Majewski, W. A., McKellar, A. R. W., Johns, J. W. C., and Watson, J. K. G., 1987, *J. molec. Spectrosc.*, **122**, 567.

[5] Watson, J. K. G., Foster, S. C., and McKellar, A. R. W., 1987, *Can. J. Phys.*, **65**, 38.

[6] Foster, S. C., McKellar, A. R. W., Peterkin, I. R., Watson, J. K. G., Pan, F.-S., Crofton, M. W., Altman, R. S., and Oka, T., 1986, *Can. J. Phys.*, **84**, 91.

[7] Amano, T., and Watson, J. K. G., 1984, *J. chem. Phys.*, **81**, 2969.

[8] Lubic, K. G., and Amano, T., 1984, *Can. J. Phys.*, **62**, 1886.

[9] Foster, S. C., McKellar, A. R. W., and Watson, J. K. G., 1986, *J. chem. Phys.*, **85**, 664.

[10] Kozin, I. N., Polyanski, O. L., and Zobov, N. F., 1988, *J. molec. Spectrosc.*, **128**, 126.

[11] Pan, F.-S., and Oka, T., 1986, *Ap. J.*, **305**, 518.

[12] MILLER, S., and TENNYSON, J., 1988, *Ap. J.*, **335,** 486.
[13] WARNER, H. E., CONNOR, W. T., PETRMICHL, R. H., and WOODS, R. C., 1984, *J. chem. Phys.*, **81,** 5214.
[14] SAITO, S., KAWAGUCHI, K., and HIROTA, E., 1984, *J. chem. Phys.*, **82,** 45.
[15] BOGEY, M., DEMUYNCK, C., and DESTOMBES, J. L., 1984, *Astr. Astrophys.*, **138,** L11.
[16] EVENSON, K., 1988 (private communication).
[17] CARNEY, G. D., and PORTER, R. N., 1974, *J. chem. Phys.*, **60,** 4251; 1976, *Ibid.*, **65,** 3547; 1977, *Chem. Phys. Lett.*, **50,** 327; 1980, *Phys. Rev. Lett.*, **45,** 537.
[18] JENSEN, P., and SPIRKO, V., 1986, *J. molec. Spectrosc.*, **118,** 208.
[19] TENNYSON, J., and SUTCLIFFE, B. T., 1984, *Molec. Phys.*, **51,** 887; 1982, *J. chem. Phys.*, **77,** 4061; 1983, *J. chem. Phys.*, **79,** 43.
[20] TENNYSON, J., and SUTCLIFFE, B. T., 1985, *Molec. Phys.*, **54,** 141.
[21] TENNYSON, J., and SUTCLIFFE, B. T., 1985, *Molec. Phys.*, **56,** 1175.
[22] TENNYSON, J., and SUTCLIFFE, B. T., 1986, *J. chem. Soc. Faraday Trans. II*, **82,** 1151.
[23] SUTCLIFFE, B. T., and TENNYSON, J., 1986, *Molec. Phys.*, **58,** 1053. TENNYSON, J., and SUTCLIFFE, B. T., 1986, *Molec. Phys.*, **58,** 1067.
[24] MILLER, S., and TENNYSON, J., 1987, *J. molec. Spectrosc.*, **126,** 183.
[25] SCHINKE, S., DUPUIS, M., and LESTER, W. A., Jr., 1980, *J. chem. Phys.*, **72,** 3909.
[26] MARTIRE, B., and BURTON, P. G., 1985, *Chem. Phys. Lett.*, **121,** 479.
[27] MEYER, W., BOTSCHWINA, P., and BURTON, P. G., 1986, *J. chem. Phys.*, **84,** 891.
[28] MILLER, S., and TENNYSON, J., 1988, *J. molec. Spectrosc.*, **128,** 530.
[29] WATSON, J. K. G., 1988 (private communication).
[30] OKA, T., 1988 (private communication).
[31] BROCKS, G., TENNYSON, J., and VAN DER AVOIRD, A., 1984, *J. chem. Phys.*, **80,** 3223.
[32] CARTER, S., and HANDY, N. C., 1987, *J. chem. Phys.*, **87,** 4294.
[33] BRINK, D. M., and SATCHLER, G. R., 1979, *Angular Momentum* (Oxford University Press).
[34] SUTCLIFFE, B. T., MILLER, S., and TENNYSON, J., 1988, *Comput. Phys. Commun.*, **51,** 73.
[35] TENNYSON, J., 1986, *Comput. Phys. Commun.*, **42,** 257.
[36] TENNYSON, J., MILLER, S., and SUTCLIFFE, B. T., 1989, *Supercomputer Algorithms for Reactivity, Dynamics and Kinetics of Small Molecules*, edited by A. Lagana (Reidel).
[37] TENNYSON, J., and MILLER, S., 1988, *Comput. Phys. Commun.* (to be submitted).
[38] STROUD, A. H., and SECREST, D., 1966, *Gaussian Quadrature Formulas* (Prentice-Hall).
[39] TENNYSON, J., 1985, *Comput. Phys. Commun.*, **38,** 39.